

P043

## Anisotropic 2.5D - 3C Finite-difference Modeling

A. Kostyukevych\* (Tesseral Technologies Inc.), N. Marmalevskyi (Ukrainian State Geological Prospecting Institute), Y. Roganov (Ukrainian State Geological Prospecting Institute) & V. Tulchinsky (Glushkov Institute of Cybernetics)

### SUMMARY

---

An example of 2.5D modeling for an anisotropic medium, by using a second order accurate central finite-difference scheme throughout the variables of the three distributed grids is demonstrated. We show an example of HTI anisotropic medium modeling for quasi-primary  $qP$ , and fast  $qS1$  and slow  $qS2$  quasi-shear waves. The time of calculation with 2.5 modeling is considerably lower than in the case of a 3D modeling for the same medium.

## Introduction

Migration procedures use finite-difference modeling of the wave elastic propagation in heterogeneous anisotropic media, to determine the spatial location of fracture, the shooting geometry design, the adjustment of interpretation algorithms and for many others cases.

However, full-wave 3D modeling is computer-intensive in time and memory. Therefore, it is difficult to be implemented even by using modern computing means such as clusters (Furumura et al., 1998)

A compromise solution could be the use of a medium model, where parameter values don't change along some direction (2.5D). For this medium, the system of differential equations that describe its wave propagation can be splitted into groups of unrelated and less complex 2D systems. The split is achieved by Fourier-transform along the invariant direction  $X_2$ . Each of the system is solved in a separate cluster node.

2.5D-modeling, as opposed to 2D-modeling, is built by using a 3D system of differential equations, and therefore the three 3D wave-field components recorded on the surface are well calculated.

The calculated wave-field contains all types of waves ( $qP, S_1$  and  $S_2$ ) created by seismic wave scattering in the medium discontinuities.

Song and William (1995) restrict the task of 2.5D acoustic modeling of a constant density medium to a linear equation system by Fourier-transform along variables  $T$  and  $X_2$  with subsequent sampling. They solve the linear equation system by LU-decomposition of the matrix representing the Helmholtz operator.

Cao and Greenhalgh (1998) derive the condition of stability, by time continuation for the same medium model. They also derive the one-way equation that they use to suppress the reflection in the model boundaries. They showed that with the fixed frequency  $k_{X_2} \neq 0$ , the propagating waves have velocity dispersion, which should be accounted for when setting the calculation parameters.

Novias and Santos (2005) presented a four order accurate finite-difference scheme along the spatial parameters and a second order accurate along the time for the same medium model and they also derived its condition of stability.

Costa and Neto (2006) proposed a 2.5D method to create a wave-field for elastic isotropic and anisotropic media. However, they only used the formulated theory for isotropic and transversely isotropic media.

In this work is presented a 2.5D finite-difference continuation scheme for a medium with arbitrary anisotropy. This scheme has a second order accuracy by all variables and is performed in rectangular grids in space and time.

## Method

Let us define  $\mathbf{u} = (u_1, u_2, u_3)^T$  to be a displacement velocity vector,  $\boldsymbol{\tau} = (\tau_{11}, \tau_{22}, \tau_{33}, \tau_{23}, \tau_{13}, \tau_{12})^T$  a stress component vector,  $\mathbf{A} = (a_{mn})$  a matrix with components of the medium stiffness tensor. Also, let us introduce the vector  $\boldsymbol{\varepsilon} = (\varepsilon_{11}, \varepsilon_{22}, \varepsilon_{33}, \varepsilon_{23}, \varepsilon_{13}, \varepsilon_{12})^T$ , where

$$\varepsilon_{11} = \frac{\partial u_1}{\partial x_1}, \quad \varepsilon_{22} = ik_2 u_2, \quad \varepsilon_{33} = \frac{\partial u_3}{\partial x_3}, \quad \varepsilon_{23} = \frac{\partial u_2}{\partial x_3} + ik_2 u_3, \quad \varepsilon_{13} = \frac{\partial u_1}{\partial x_3} + \frac{\partial u_3}{\partial x_1}, \quad \varepsilon_{12} = ik_2 u_1 + \frac{\partial u_2}{\partial x_1}.$$

After Fourier-transform along the variable  $X_2$ , the equations for the elastic wave propagation in an anisotropic medium can be presented as:

$$\frac{\partial}{\partial t} \begin{pmatrix} u_1 \\ u_2 \\ u_3 \end{pmatrix} = \frac{1}{\rho} \begin{pmatrix} \tau_{11} & \tau_{12} & \tau_{13} \\ \tau_{12} & \tau_{22} & \tau_{23} \\ \tau_{13} & \tau_{23} & \tau_{33} \end{pmatrix} \begin{pmatrix} \frac{\partial}{\partial x_1} \\ jk_2 \\ \frac{\partial}{\partial x_3} \end{pmatrix} + \mathbf{f} ,$$

$$\frac{\partial \boldsymbol{\tau}}{\partial t} = \mathbf{A}\boldsymbol{\varepsilon} + \mathbf{M} , \quad (1)$$

where  $\mathbf{f}$  and  $\mathbf{M}$  are sources of force density and moments of force, respectively.

All components of vectors  $\mathbf{u}$  and  $\boldsymbol{\tau}$  are located in three rectangular grids with mutual displacements  $\Delta \mathbf{x}_1 / 2$  and  $\Delta \mathbf{x}_3 / 2$  in relation with their denominations:  $\{\tau_{11}, \tau_{22}, \tau_{33}, u_2\} \subset \mathbf{R}_{00}$ ,  $\{\tau_{23}, u_3\} \subset \mathbf{R}_{\Delta x_1 / 2, 0}$  and  $\{\tau_{12}, u_1\} \subset \mathbf{R}_{0, \Delta x_3 / 2}$ .

The values of the auxiliary variables  $\varepsilon_{ij}$  are calculated in those grid places, where is necessary to obtain  $\frac{\partial \tau_{ij}}{\partial t}$ . To accomplish this, linear interpolations are sometimes performed

$$\varepsilon_{ij}^p(\mathbf{x}) = 0,5[\varepsilon_{ij}(\mathbf{x} - \Delta x_p / 2) + \varepsilon_{ij}(\mathbf{x} + \Delta x_p / 2)],$$

$$\varepsilon_{ij}^{pq} = (\varepsilon_{ij}^p)^q .$$

The finite-difference scheme is achieved by sampling the analytical relation (1) and it is central with regard to all variables.

The sample interval selection is determined by the stability conditions of the finite-difference scheme and the acceptable dispersion in the frequency interval of the signal. For distributed grids, like those used in this work, the stability condition of the scheme is covered in article (Saeger and Bohlen, 2004).

The wave-field related to the point  $M(x_1, x_2, x_3)$  is determined by the formula

$$\mathbf{u}(x_1, x_2, x_3, t) = \sum_{k_2} \exp(ik_2 x_2) \mathbf{u}(x_1, k_2, x_3, t).$$

## Numerical examples

When performing 2D full-wave modeling, the anisotropic medium must have a symmetry plane, and the survey line must lie within this plane. Therefore, there is not a way of modeling the wave propagation for a medium with a fracturing system that leads to an absence of the mentioned above axial plane. This limitation does not exist in 2.5D modeling

Let us have a model consisting of two HTI anisotropic layers with the following parameters: the upper layer anisotropic axis is located in the plane  $X_1 X_3$ , and the lower one has an azimuth of  $45^\circ$ .

The source has a frequency of 40 Hz and generates qP and qSV ( $S_2$ ) waves. Geophones are located every 10 m.

Upper layer parameters: quasi-compressional wave velocity along the symmetry axis of HTI-medium is  $V_{p1}=3000\text{m/c}$ , quasi-shear wave velocity  $V_{s1}=2000\text{m/c}$ , density  $\rho_1=2200\text{m/c}$ , Thomsen's parameters  $\varepsilon_1=0.1$ ,  $\delta_1=0.15$ ,  $\nu_1=0.2$ .

Lower layer parameters: same designations but with index 2.  $V_{p2}=3500\text{m/c}$ ,  $V_{s2}=2400\text{m/c}$ ,  $\rho_2=2300\text{m/c}$ ,  $\varepsilon_2=0.1$ ,  $\delta_2=-0.1$ ,  $\nu_2=0.2$ .

The specifics of this model are that in the upper layer, the source only generates downward traveling qP and  $S_2$  waves. In this case a  $S_1$ - wave is not generated, since the source does not generate oscillations in the plane perpendicular to the axis of anisotropy of the HTI upper medium. At the boundary between two layers qP- $S_1$ , qP- $S_2$  and  $S_2$ - $S_1$ ,  $S_2$ -qP waves are generated and they travel upward and downward from this boundary. Considering the direction of the upper layer axis of anisotropy, fast converted waves will be recorded at surface on the  $U_2$  component, and qP and  $S_2$  polarization waves will be recorded on the  $U_1$  and  $U_3$  components. At the same time, in the lower layer all type of waves have non-zero amplitudes on all three components, since the axis of anisotropy has an azimuth of  $45^\circ$

In Fig. 1. are shows a wave-field section obtained on components  $U_1$  (Fig. 1a),  $U_2$  (Fig. 1b) and  $U_3$  (figure. 1c) at the time  $t=0.06s$ . By this time, on the  $U_2$  (Fig. 1b) component the wave field is equal to zero, since downward waves haven't reached the reflection boundary yet. All wave types are shown by arrows in the wave-fields pictures.

In Fig. 2 are shows wave-field sections for time  $t=0.28s$ . By this time, both qP and  $S_2$  waves have already reached the reflection boundary and originated downward and upward waves of all types: qP-qP, qP- $S_1$ , qP- $S_2$ ,  $S_2$ - $S_2$ ,  $S_2$ - $S_1$   $S_2$ -qP. As mentioned above, in the lower layer, these waves have non-zero energy on all three components. In the upper layer, different quasi-shear waves have energy on the different components.

In Fig. 3. are displays a multi-component seismogram recorded at the survey surface. By comparing the arrival times of the quasi-shear waves to the different components, we can see that the quasi-shear wave on component  $U_2$  propagates faster than the quasi-shear waves recorded on components  $U_1$  and  $U_3$ .

This basic model was chosen just for convenience, since it easily illustrates the different types of waves. 2.5D modeling correctly calculates the wave-fields for media of any complexity in the plane  $X_1X_3$  and with any type of layer anisotropy. For example, a medium can have a triclinic anisotropy type.

## Conclusions

We illustrated an example of 2.5D modeling for anisotropic medium. The calculation was performed by using a second order accurate central finite-difference scheme along all variables on the three distributed grids. It was shown as well a way of modeling waves of all types of polarization for an HTI medium.

## References

- Cao, S. and Greenhalgh, S. [1998] 2.5D modeling of seismic wave propagation: Boundary condition, stability criterion, and efficiency. *Geophysics*, **63**, 2082-2090.
- Costa, J., and Neto, F. [2006] 2.5D Elastic finite-difference modeling. *EAGE 68<sup>th</sup> Conference and Exhibition*, P034.
- Furumura, T., Kennet, B., and Takenara, H. [1998] Parallel 3-D pseudospectral simulation of elastic wave propagation. *Geophysics*, **63**, 279-288.
- Neto, F., and Costa, J. [2006] 2.5D anisotropic elastic finite-difference modeling. *76<sup>th</sup> SEG Annual Meeting*, Expanded Abstracts, 2275-2279.
- Novias, A. and Santos J. [2005] 2.5D finite-difference solution of the acoustic wave equation. *Geophysical Prospecting*, **53**, 523-531.
- Saeger, E. and Bohlen, T. [2004] Finite-difference modeling of viscoelastic and anisotropic wave propagation using the rotated staggered grid. *Geophysics*, **69**, 583-591.
- Song, Z. and Williamson, F.R. [1995] Frequency – domain acoustic-wave modeling and inversion of cros-hole data: Part 1 -2.5-D modeling method. *Geophysics*, **60**, 784-795.

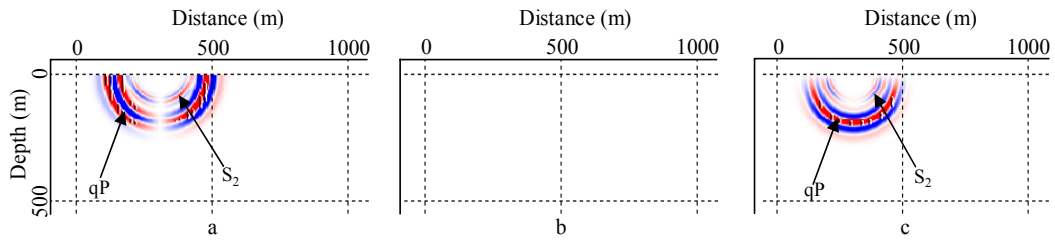


Figure 1. Wave-field components for time  $t=0.06c$  (a)  $U_1$  – component, (b)  $U_2$  – component, (c)  $U_3$  – component.

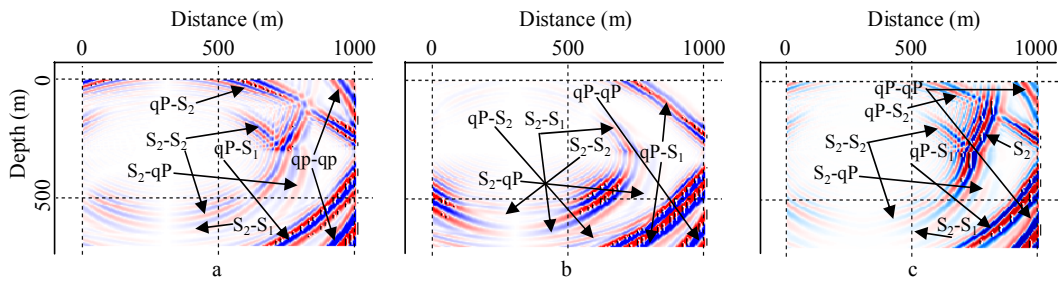


Figure 2. Wave-field components for time  $t=0.28c$  (a)  $U_1$  – component, (b)  $U_2$  – component, (c)  $U_3$  – component.

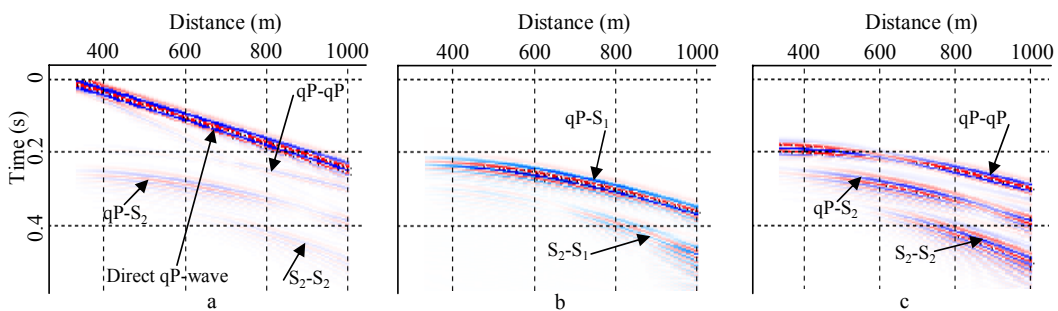


Figure 3. Multi-component seismogram (a)  $U_1$  – component, (b)  $U_2$  – component, (c)  $U_3$  – component.